



AIAA-2000-1950

**Experimental Impedance of Single Liner
Elements with Bias Flow**

J. I. Follet
University of Virginia
Virginia Consortium of Engineering and Science Universities
Hampton, VA 23666

J. F. Betts and J. J. Kelly
Virginia Tech
Virginia Consortium of Engineering and Science Universities
Hampton, VA 23666

and

R. H. Thomas
NASA Langley Research Center
Hampton, VA 23681

**6th AIAA/CEAS
Aeroacoustics Conference
12-14 June 2000 / Lahaina, Hawaii**



EXPERIMENTAL IMPEDANCE OF SINGLE LINER ELEMENTS WITH BIAS FLOW

Jesse I. Follet*, Juan F. Betts†, and Jeffrey J. Kelly‡
 University of Virginia
 Virginia Consortium of Engineering and Science Universities
 303 Butler Farm Road, Suite 101
 Hampton, Virginia 23666

Russell H. Thomas§
 NASA Langley Research Center
 Hampton, VA 23681

Abstract

An experimental investigation was conducted to generate a high quality database, from which the effects of a mean bias flow on the acoustic impedance of lumped-element single-degree-of-freedom liners was determined. Acoustic impedance measurements were made using the standard two-microphone method in the NASA Langley Normal Incidence Tube. Each liner consisted of a perforated sheet with a constant-area cavity. Liner resistance was shown to increase and to become less frequency and sound pressure level dependent as the bias flow was increased. The resistance was also consistently lower for a negative bias flow (suction) than for a positive bias flow (blowing) of equal magnitude. The slope of the liner reactance decreased with increased flow.

Introduction

Because communities are impacted by steady increases in aircraft traffic, aircraft noise continues to be a growing problem for the growth of commercial aviation. Research has focused on improving the design of specific high-noise source areas of aircraft and on noise control measures to alleviate noise radiated from aircraft to the surrounding environment. Engine duct liners have long been a principal means of attenuating the turbo-machinery portion of engine noise. The ability to control in-situ the impedance of a liner would

provide a valuable tool to improve the performance of liners. Increased attenuation rates, the ability to change liner impedance to match various operating conditions, or the ability to tune a liner to more precisely match design impedance represent some ways that in-situ impedance control could be useful.

The research to be presented in this paper deals with a set of experiments that were performed to provide the basis for improving the understanding and ability to predict bias flow effects on the impedance of liner elements. The experimental database presented herein was produced using the methods described in this study and fully presented by Kelly et al.¹

This work can be compared to two recent bias flow liner studies, specifically that of Premo² and Cataldi, Ahuja, and Gaeta³. Premo developed a time-domain impedance model that included the effects of bias flow, and compared it with measured bias flow liner data. Cataldi looked specifically at the sound absorption of liners with negative bias flow or suction.

A companion paper⁴ uses the experimental database presented herein as a basis for evaluating liner impedance models that include bias flow effects.

Testing Facility

The NASA Langley Normal Incidence Tube (NIT) was used to make impedance measurements of lumped-element single-degree-of-freedom liners with bias flow (see Figure 1). Six acoustic drivers generate an

* Graduate Research Assistant, Department of Mechanical and Aerospace Engineering, University of Virginia, Member AIAA.

† Graduate Research Assistant, Mechanical Engineering Department, Virginia Polytechnic Institute and State University, Member AIAA.

‡ Research Associate Professor, Mechanical Engineering Department, Virginia Polytechnic Institute and State University, Senior Member AIAA.

§ Aerospace Engineer, Aeroacoustics Branch, NASA Langley Research Center, Senior Member AIAA.

Copyright©2000 by the American Institute of Aeronautics and Astronautics, Inc. No copyright is asserted in the United States under Title 17, U.S. Code. The U.S. Government has a royalty-free license to exercise all rights under copyright claimed herein for Governmental Purposes. All other rights are reserved by the copyright owner.

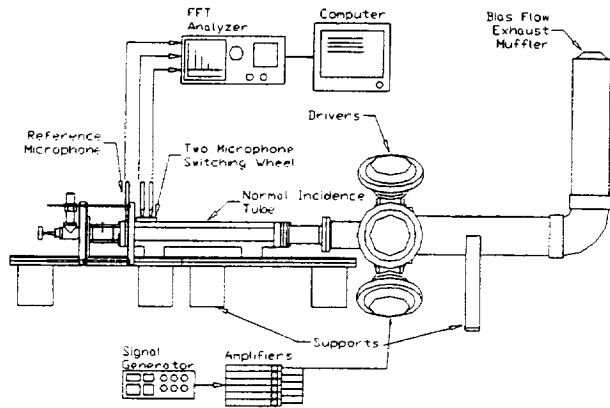


Figure 1. Schematic description of NASA Normal Incidence Tube with modifications to allow for bias flow. One-degree-of-freedom liner installed at left end.

acoustic plane-wave pressure field which, upon reflection from the perforate sample, sets up a standing wave along the axis of the 5.08-cm square tube. The perforate facesheet sample is placed at the end of the tube and backed with a short 5.08-cm square cavity. This cavity is terminated with a high resistance fibermetal sheet designed to allow mean flow to pass through while reflecting almost all the acoustic signal. Three microphones are used in the test procedure. The microphone nearest the specimen is stationary, and is used to measure the sound pressure level near the surface of the specimen. Two other microphones measure the frequency dependent transfer functions (acoustic pressure magnitude and phase differences) between their respective locations. This information is equivalent to determining the standing wave pattern in the tube. Since the acoustic wave patterns are related to the surface impedance of the perforate-cavity system (test specimen), this impedance can then be determined.^{5,6}

The surface impedance of the specimen is given by

$$\xi = \frac{1+R}{1-R} = \theta - i\chi \quad (1)$$

where R is the complex reflection coefficient,

$$R = \frac{P_r}{P_i} \quad (2)$$

and θ and χ are the normalized resistance and reactance, respectively.

A signal generator is used to generate discrete frequency signals that are input to the power amplifiers. The amplified signals are then input to the acoustic drivers. Signals from the microphones are sampled and averaged using an FFT analyzer and the data is stored on the computer.

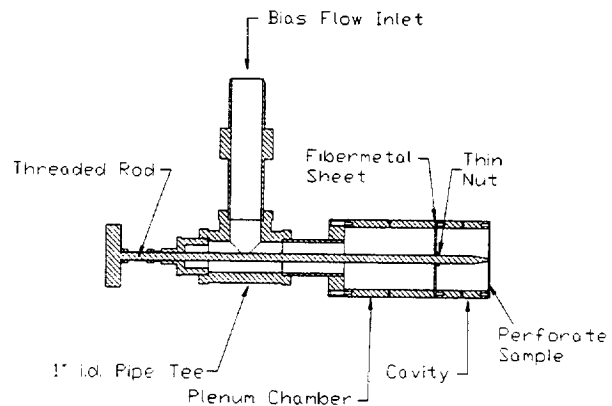


Figure 2. Schematic of hardware to supply mechanical support and bias flow to perforate sample.

Positive bias flow (blowing) is introduced through the 2.54-cm diameter inlet tee, shown in Figure 2, into a 5.08-cm square plenum chamber. The flow then continues through a high resistance (at least 10 pc) fibermetal sheet into the cavity section and through the perforate sample. The flow is exhausted through the muffler depicted in Figure 1. Negative bias flow (suction) is generated by replacing the pressure source with a vacuum pump, thereby reversing the direction of the flow. A reference sample was tested in the NIT before and after the muffler was installed. Results showed the muffler had no effect on the measured impedance.

To adequately measure and control the bias flow velocity in each section, four pressure ports were installed along the sides of each duct section before and after each major pressure drop in the bias flow liner. To measure the velocity through each section, mass continuity and the ideal gas equation are used:

$$\rho_k V_k A_k = \rho_{k+1} V_{k+1} A_{k+1} \quad (3)$$

$$\rho_k = \frac{P_k}{RT}$$

Here the index k indicates the section number (see Figure 2) and ρ , V , P , R , and T are the density, velocity, absolute pressure, ideal gas constant, and temperature, respectively. The mass flow is measured with a laminar flow meter upstream of the inlet tee. Using equation 4, the velocity is calculated in each section.

Plate Resonance

Contamination of the intrinsic perforate impedance by a "shunt impedance" due to plate vibration is a

recurrent problem in measurements of this type⁷. For this study, shunt impedance effects were clearly evident for some of the perforate samples. Consequently, special precautions were taken to inhibit this contamination. The measured impedance is always a combination of the plate mechanical impedance and the liner acoustic impedance, which can be modeled as parallel, lumped impedances. For most cases, the plate mechanical impedance is high enough, relative to the liner acoustic impedance, to cause minimal contamination. Near the plate mechanical resonance, however, it becomes a significant factor; i.e., in the range of the perforate impedance.

Near the resonant frequency of the plate, the impedance is transitioning from a stiffness-dominant to a mass-dominant system. Therefore, to counter resonance behavior exhibited in the acoustic impedance measurements, the plate stiffness was increased. This was achieved by the addition of a post support mechanism. Figure 3 shows a comparison of the acoustic impedance spectra for a single perforate sample when it is mounted with or without the post support mechanism. The unsupported plate (no post support) spectra show the resonance frequency behavior, with a drop in impedance above the resonance frequency. The addition of the post support causes the structural resonance of the plate (perforated sheet sample) to shift to a higher frequency, above 3 kHz; thus, the resultant spectra is uncontaminated by plate resonance behavior in the current frequency range of interest.

In typical aircraft applications, this desired stiffness is achieved by permanently bonding a cellular honeycomb to the perforate sample. However, the honeycomb walls and the bonding agent cause perforate hole blockage. Since the purpose of this study was to study the effects of bias flow on the perforate, this blockage was unacceptable. Also, keeping the perforated plates unbonded allowed simple interchange of test materials. In contrast, the post blocked no more than one hole and it accounted for only 1.25% of the total cross-sectional area of the cavity.

Figure 2 shows the post support mechanism. The post was centered through the fibermetal termination face into the cavity until it pushed against the perforate sample. A thin nut was installed on one side of the fibermetal to secure the fibermetal firmly.

Perforate Description

Each perforate was specially fabricated for this set of experiments. The samples are 6.35-cm square perforated plates, with rounded corners to conform to the NIT sample holder. The geometric parameters (plate thickness, hole diameter, and percent open area), as

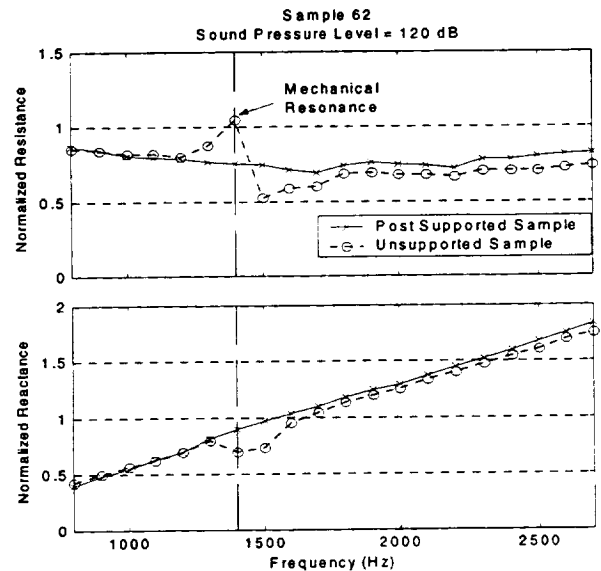


Figure 3. Example of structural resonance affecting liner impedance.

depicted in Figure 4, were varied for these plates over the respective ranges of

$$0.24 \text{ mm} < d < 1.48 \text{ mm}$$

$$0.51 \text{ mm} < t < 1.02 \text{ mm}$$

$$0.9\% < \text{POA} < 16.5\%$$

Table 1 gives the target and measured dimensions for the perforate liner samples. The target dimensions were chosen such that only one perforate dimension was varied at a time. Due to fabrication inconsistencies, the measured dimensions are slightly different from the desired values. The numbers quoted in the table represent an average of several measurements, with each standard deviation being within $\pm 2\%$ of the mean. The ranges of perforate dimensions were chosen to encompass what is typically seen in aircraft engine liners. Several groups of 5-15 POA perforates with constant plate thickness and hole diameter were selected. One group of 1-5 POA perforates was also selected.

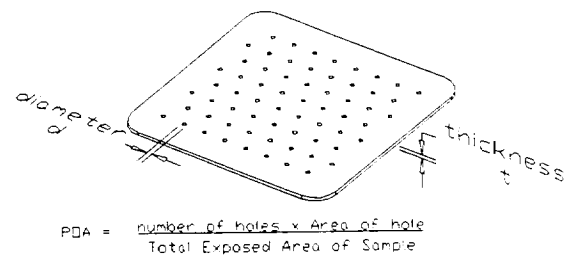


Figure 4. Geometric parameters of liner perforates.

A microscope was used to measure the individual hole diameters. Thirty holes were examined for the initial perforate. An analysis of those results concluded that only ten holes needed to be measured for successive samples. Perforate sheet thickness was measured using a micrometer, and the POA was determined by multiplying the number of holes in the perforate by the cross-sectional area per hole, then dividing by the total area of the sheet (5.08-cm square) exposed to the acoustic field in the NIT. As shown in the table, the fabrication process was better for the 5-15 POA perforates than for the 1-5 POA perforates.

Table 1. Target and measured dimensions for fabricated perforated sheets.

Sample #	Hole Depth, d (mm)		Sheet Thickness, t (mm)		Percent Open Area, POA (%)	
	Target	Meas	Target	Meas	Target	Meas
43	0.61	0.64	0.64	0.64	5	5.7
44	0.61	0.63	0.64	0.66	10	10.5
45	0.61	0.60	0.64	0.69	15	14.5
46	0.88	0.92	0.64	0.64	5	5.4
47	0.88	0.92	0.64	0.64	10	10.7
48	0.88	0.91	0.64	0.61	15	15.6
49	1.02	1.04	0.64	0.64	5	5.3
50	1.02	1.03	0.64	0.64	10	10.2
51	1.02	1.03	0.64	0.64	15	15.5
52	0.61	0.66	1.02	0.99	5	5.9
53	0.61	0.64	1.02	0.97	10	10.9
54	0.61	0.64	1.02	1.02	15	16.5
55	1.02	1.05	1.02	0.97	5	5.4
56	1.02	1.04	1.02	1.02	10	10.3
57	1.02	1.05	1.02	0.97	15	16.0
58	1.40	1.48	1.02	0.99	5	5.7
59	1.40	1.47	1.02	1.02	10	11.0
60	1.40	1.46	1.02	1.02	15	16.6
61	0.25	0.24	0.46	0.53	1	0.9
62	0.25	0.26	0.46	0.51	2	2.2
63	0.25	0.26	0.46	0.51	3	3.1
64	0.25	0.29	0.46	0.51	4	5.2
65	0.25	0.28	0.46	0.51	5	6.1

Non-Switching Two-Microphone Method

The NIT facility has traditionally utilized a switching two-microphone method⁶ (S-TMM) that involves acquiring transfer function data between two microphone locations. The transfer functions between the two microphones are measured before and after the microphone positions are very accurately swapped by the usage of a rotating microphone plug. Appropriate averaging of the two readings eliminates the effects of any magnitude and phase differences between the two microphones. When this method is used with a discrete frequency source, the microphones must be swapped

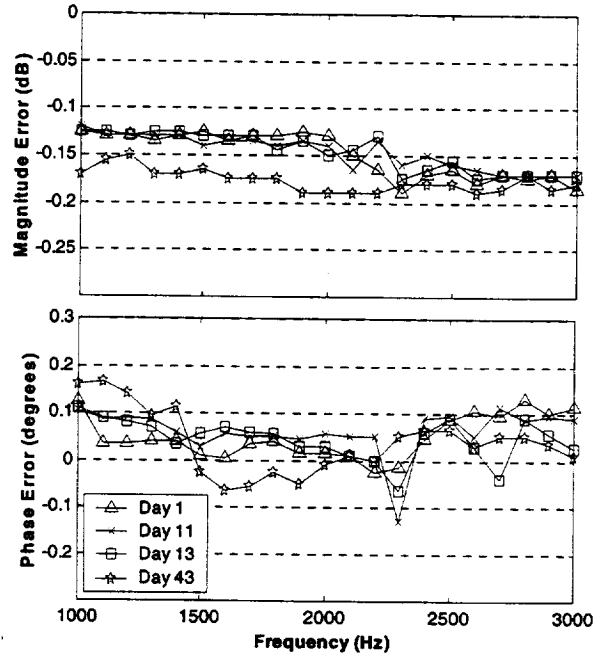


Figure 5. Magnitude and phase calibration constants for the non-switching method measured over a period several days to one month apart.

for each source frequency. While this eliminates the need for a separate calibration procedure, it is inefficient for the testing of a large number of test specimens. Thus, a modified version of the standard Two-Microphone Method^{8,9}, which does not require microphone switching during the test process, was used to significantly shorten the acquisition duration. This technique will be referred to as the Non-Switching Two-Microphone Method (NS-TMM).

Proper implementation of the NS-TMM method requires accurate amplitude and phase calibration, for each microphone, across the entire frequency range of interest. To accomplish this, the plug containing two measurement microphones was rotated such that the microphones were positioned in a plane perpendicular to the duct axis. For frequencies below cut-on for the first higher order mode, measured amplitude or phase differences between the microphones are due to inherent differences between the microphones and signal conditioning. To account for these differences, the averaging process of the S-TMM method was used to acquire calibration constants at each frequency. These calibration constants were then used in the NS-TMM impedance determination method.

Figure 5 depicts the variability of the calibrations over an extended period of time. The magnitude calibration constants vary little from day to day, but over the course of the test there was a variability of approximately 0.1 dB. The phase calibration constants

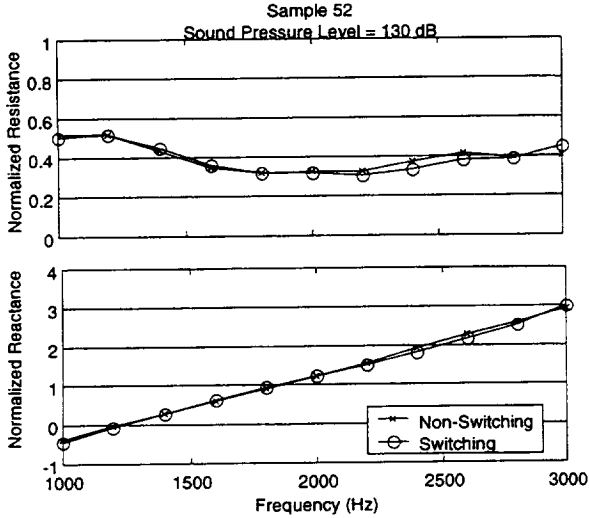


Figure 6. Sample impedance data comparing NS-TMM and S-TMM.

have somewhat more variability (approximately 0.3 degrees). Thus, for improved quality, calibration constants were acquired daily for the experimental database presented here.

Figure 6 shows a comparison of results acquired with the NS-TMM and S-TMM methods for a typical perforate liner. The results are almost identical. In fact, repeatability tests to be discussed later demonstrate more variability than shown here. Thus, the NS-TMM was determined to be acceptable for the current tests.

Repeatability and Error Estimation

To ensure data quality, Perforates 52-54 and 62 were used to conduct repeatability tests. These samples were each tested four times over the frequency range of 1300 to 2200 Hz (100 Hz increments) for SPL's of 100, 120 and 140 dB. These four perforates were used to represent the repeatability error for the full range of percent open areas being tested, with no bias flow. Thus, while providing helpful information regarding the NS-TMM method, these results do not offer proof of the quality of the results acquired with bias flow. A repeatability analysis is planned for bias flow testing, and will be reported in a future paper.

For an individual sample at a fixed SPL, the mean acoustic resistance (similarly, for acoustic reactance) was computed from four measurements at each frequency. The percentage deviations (PD's) from the mean were then computed for each of the four measurements. Thus, for ten frequencies at four measurements per frequency, this gave 40 PD's. These 40 values of PD's were used to compute a global

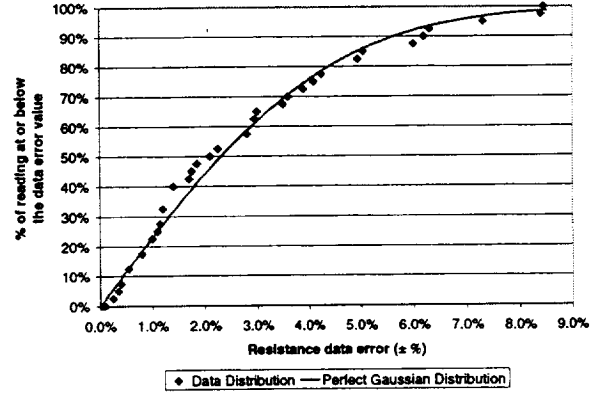


Figure 7. Comparison of ideal Gaussian probability distribution function and data distribution (SPL of 100dB, 5 POA)

standard deviation for the selected sample and SPL, using

$$s = \sqrt{\frac{\sum_{i=1}^N (x_i - \bar{x})^2}{N - 1}} \quad (4)$$

where x_i is the individual PD and $N=40$. Since the focus of this analysis was to quantify the repeatability (random) error, \bar{x} was set to zero; i.e., the systematic error was ignored. The total error from the mean (% of data lying within 95% of the mean), which is $\pm 2s$, is provided in Table 2 for each sample and SPL.

A comparison of the Gaussian probability distribution with the measurement data (PD's discussed above) is shown in Figure 7.¹⁰ This figure shows the percentage of data lying below a certain mean for both the ideal Gaussian distribution and the measured data. Clearly, the distribution is "near" Gaussian in nature; thus, computing the repeatability error using the Gaussian mean and standard deviation should be sufficient for characterization of this data. Figure 7 also shows that 95% of the data is within $\pm 7.25\%$ of the mean.

Table 2 provides repeatability data for all of the samples, at each of the three SPL's tested. All twenty-four data sets show similar evidence of "near" Gaussian distributions of data. The measured data are shown to be off the mean value by a maximum of 7%. It should be noted that only 32 averages are sampled by the FFT analyzer for each microphone signal. In order to reduce data uncertainty, the number of averages could be increased. Regardless, with the data given in Table 2, it is reasonable to assume that overall measurement error is at most $\pm 7\%$.

Table 2. Data acquisition repeatability percent error for tests conducted with no bias flow

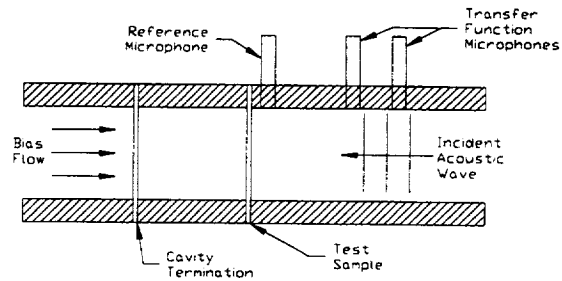
Resistance				
SPL	1-3 POA	4-7 POA	8-12 POA	13-17 POA
100 dB	±5%	±7%	±6%	±7%
120 dB	±6%	±7%	±6%	±7%
140 dB	±7%	±5%	±5%	±5%
Reactance				
100 dB	±2%	±2%	±4%	±2%
120 dB	±4%	±2%	±3%	±4%
140 dB	±7%	±3%	±5%	±7%

High Resistance Fibermetal:
Impedance Determination

For the purposes of this study, it was important to design the experiment such that the bias flow effect on perforate samples could be analyzed with locally-reacting acoustic liner models. To achieve this, one of the key elements of the bias flow liner is the termination at the back of the cavity. For passive liners, the termination face for the acoustic wave in the cavity is a highly reflective surface. To add bias flow, this termination must be permeable while maintaining high reflectivity. A high resistance fibermetal was chosen to achieve this condition. Fibermetal is a dense mesh of metallic strands pressed and bonded together.

Premo² also used this approach, specifically applying a backing sheet with a nominal flow resistance of 190 cgs Rayls at 105 cm/s. There was no mention of whether this value was verified; however, his results showed an 0.3 pc resistance difference from the hardwall measurement, which indicated the backing layer resistance was not large enough to adequately simulate a hardwall.

Four different methods were used to evaluate the high resistance fibermetal sheet used in this experiment. In most acoustic liner models, the flow resistance (sometimes referred to as the direct current, or DC, flow resistance) is assumed to be equal to the acoustic resistance at low frequencies. As described below, the first three methods determine the acoustic resistance using complex acoustic pressure measurements in the normal incidence impedance tube. Of these, the first is an indirect method, which requires that the acoustic resistance be deduced from measurements of multiple configurations. The other two methods allow the acoustic resistance to be determined directly. Figure 8 contains a summary sketch listing all of the components used in each of these tests. The last method uses a laser velocimeter to measure the flow resistance.



Indirect Method

Test 1:

Test Sample: Perforate sheet
Cavity Termination: Hardwall
Bias Flow: Off

Test 2:

Test Sample: Perforate sheet
Cavity Termination: High resistance fibermetal sheet
Bias Flow: On

Direct Method I

Test Sample: High resistance fibermetal sheet
Cavity Termination: Hardwall
Bias Flow: Off

Direct Method II

Test Sample: Open (no sample installed)
Cavity Termination: High resistance fibermetal sheet
Bias Flow: On

Figure 8. Summary sketch of three methods used to determine acoustic resistance of fibermetal sheet.

Indirect Acoustic Method

A low resistance perforate was tested in the normal incidence tube using two configurations. For the first configuration, the perforate had a cavity with a hardwall termination. For the other, the termination was the high resistance fibermetal under investigation, which could allow bias flow to be passed through the tube. Using the NS-TMM method described earlier, the acoustic impedance of the perforate sample was determined for each of these configurations.

The impedance measured at the surface of the perforated plate for the hardwall termination is given as ξ_{s1} . Similarly, the impedance measured with the fibermetal termination is ξ_{s2} . These two impedances are the sum of the individual impedances of each liner element; i.e.,

$$\xi_{s1} = \xi_p + \xi_{cw} \quad (5)$$

$$\xi_{s2} = \xi_p + \xi_{cf} \quad (6)$$

where ξ_p is the perforate impedance, and ξ_{cw} and ξ_{cf} are the cavity impedances with the hardwall and

fibermetal terminations, respectively. For this method to work ξ_p must be independent of the test configuration. The only way to assure ξ_p is constant is for the perforate to be linear (independent of SPL and bias flow). Tests were conducted over the bias flow and SPL range of interest in this study with the high resistance fibermetal termination installed. The results of these tests indicated that the selected perforate sample was acceptably linear.

Subtracting equation 6 from 7 and solving for ξ_{cf} produces

$$\xi_{cf} = \xi_{cw} + \xi_{s2} - \xi_{s1} \quad (7)$$

This is the cavity impedance with the fibermetal backing. The cavity impedance due to the hardwall is given by

$$\xi_{cw} = -iCot(kL) \quad (8)$$

where L is the cavity length, and k the wave number. The lumped-element impedance of the fibermetal ξ_f is related to the cavity impedance with the fibermetal termination ξ_{cf} by the following relationship

$$\xi_f = -\frac{(\xi_{cf} - 1)e^{i(k_i + k_r)L} + (\xi_{cf} + 1)}{(\xi_{cf} - 1)e^{i(k_i + k_r)L} - (\xi_{cf} + 1)} \quad (9)$$

where the wave numbers k_i and k_r are

$$\begin{aligned} k_i &= \frac{k}{1+M} \\ k_r &= \frac{k}{1-M} \end{aligned} \quad (10)$$

and M is the Mach number in the duct.

The major advantage of this method is that ξ_{s1} and ξ_{s2} can be measured accurately. Measurements near nulls of large standing waves are avoided by properly choosing the perforate material, consequently improving the accuracy of the measurement. Perhaps more importantly, bias flow effects on the fibermetal impedance can be studied. The major disadvantage of this method is that more measurements and calculations are required to determine the impedance of the fibermetal.

Direct Acoustic Methods

There are two ways to measure the fibermetal impedance directly. In Method I the fibermetal sheet under investigation is installed as the "test sample" in the NIT, with a hardwall termination. The NS-TMM method is then used to measure the normal incidence acoustic impedance. This method offers the advantage of requiring only a single measurement, and consequently is a fast method for determining the impedance properties of the fibermetal. Its main disadvantage is the inability to measure how bias flow affects the fibermetal impedance.

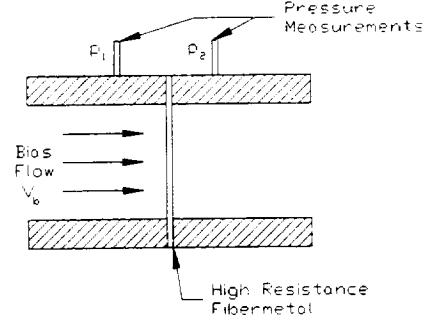


Figure 9. Raylometer experimental setup for determining fibermetal resistance (Raylometer Method).

In Method II the fibermetal under investigation is used as the cavity termination. For this method, no sample is installed; thus, the cavity is left open. The fibermetal impedance is determined using equation 10, where ξ_{cf} and ξ_f are the measured impedance at the standard test plane (where sample surface is typically located) and fibermetal lumped-element impedance, respectively. The advantage of Method II is the single-step process in measuring the impedance of the fibermetal. Furthermore, this method allows for the determination of bias flow effects on the impedance of the fibermetal. The major disadvantage to this method is the potential for measuring near nulls of large standing waves, with the accompanying increased potential for measurement error due to large changes in SPL over the diameter of the measurement microphone.

Raylometer Method

The raylometer measures the DC flow resistance of the high resistance fibermetal backing. Figure 9 shows the typical experimental setup utilized for this experiment. The non-dimensional resistance, θ , is

$$\theta = \frac{p_1 - p_2}{\rho c V_b} \quad (11)$$

where p_1 , p_2 , V_b , ρ , and c are the pressure reading before the fibermetal, pressure reading after the fibermetal, velocity in the duct, fluid density, and the speed of sound, respectively. The flow resistance is assumed to be a linear function of velocity of the form

$$\theta = A + B \frac{V_b}{c} \quad (12)$$

Several values of flow resistance versus flow velocity were acquired in this experiment. These values were then curve-fitted to determine A and B.

The advantage of using the raylometer is the speed of acquiring the data. The disadvantage is the assumption that the resistance of a DC flow measurement is equivalent to the real part of the

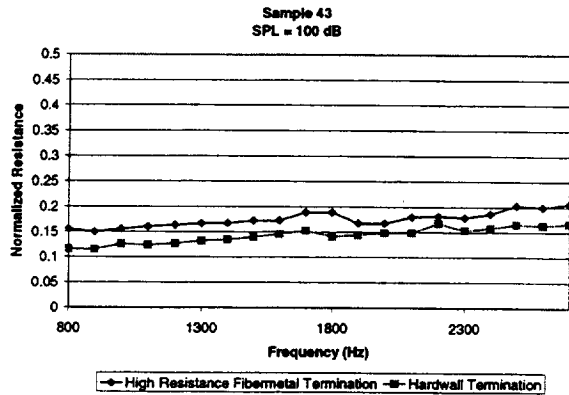


Figure 10. Measured difference between the hardwall termination and the high resistance fibermetal termination.

acoustic impedance. This assumption is not entirely correct because frequency dependence is ignored.

Fibermetal Resistance

The measured flow resistance of the fibermetal using the raylometer was 1200 cgs Rayls at 105 cm/s. This is much larger than the manufacturer's quoted value of 550 cgs Rayls. It is also substantially larger than 190 cgs Rayls, which was the flow resistance of the material used by Premo in a similar test.

The acoustic impedance measurements of the fibermetal consistently showed the acoustic resistance to be around 20 pc. Thus, it was expected to provide sufficiently high acoustic reflection to simulate a rigid termination. Figure 10 shows the acoustic resistance measured for a selected sample liner (Sample 43) with the high resistance fibermetal termination versus that measured with a hardwall (highly reflecting) termination. The high resistance fibermetal termination causes the acoustic resistance to be slightly higher in magnitude (~ 0.05 pc) than that with the hardwall termination. This is significantly lower than the 0.3 pc error observed by Premo. The measured acoustic reactance (not shown) of the sample liner was unchanged for each type of termination.

Results

The acoustic impedance was measured for each perforate described in Table 1 with a constant cavity depth of 2.72 cm, which has a resonance near 2 kHz. The cavity depth was chosen to minimize cavity reactance and avoid anti-resonance over the testing frequency range of 1 to 3 kHz. These measurements were conducted for SPL's of 120, 130 and 140 dB, as measured by the reference microphone near the surface of the perforate. The bias flow rates were set to 0, 100,

200, 300 and 600 cm/s for each perforate, and a selected number of perforates were also tested at -25, 25 and 50 cm/s. These flow rates are comparable to those investigated by Premo and Cataldi, et.al.; however, neither had looked at the high flow rate of 600 cm/s and Cataldi investigated only negative bias flow (suction).

The measured impedances for each of the perforate samples were included in the analysis. For the sake of brevity, only a few important data sets will be shown and described in terms of their significance. The full data set is presented in reference 1.

The first significant result is the effect of bias flow on the acoustic nonlinearity of the perforate samples. The acoustic nonlinearity is the dependence of the impedance on sound pressure level. Figure 11 shows how increasing the sound pressure level increases and changes the trend with frequency of the normalized resistance in the absence of bias flow. Figure 12 provides data acquired with a bias flow of 50 cm/s, and shows how the resistances at 120 and 130 dB are the same in magnitude and frequency trend. However, at 140 dB the resistance is significantly increased over the frequency range of 1 to 2 kHz, yet remains virtually unchanged relative to the data acquired at 120 and 130 dB at higher frequencies. Figure 13 shows how bias flow increases the resistance, eliminates its dependence to sound pressure level, and reduces its dependence on frequency. This is an important result, since it indicates that it is possible to achieve constant impedance for all sound pressure levels at a particular frequency. Therefore, a model of this effect becomes greatly simplified. The reactance is independent of sound pressure level for these three cases.

Figure 14 shows the effects of bias flow rate on the impedance. As the bias flow rate is increased, the reactance tends to decrease in slope until it becomes almost flat, at which point the measured data seem to deviate from a steady trend. As expected, the resistance increases with increasing bias flow rate. It should be pointed out that the acoustic resistance for a bias flow rate of 600 cm/s is on the order of 8 to 9 pc, which is near the limits of typical impedance measurements in the NASA Langley Normal Incidence Tube. Thus, that data may be suspect.

As Figure 15 shows, the resistance tends to increase almost linearly for bias flow rates of 25 to 300 cm/s. Recall that at low flow rates the acoustic resistance is highly nonlinear with respect to SPL. This figure also indicates that the resistance is nonlinear with bias flow at high bias flow rates. The normal incidence impedance for the high bias flow rates warrants further investigation in both measurement certainty and physical modeling. It should be noted that Premo shows similar trends in acoustic resistance versus bias flow rate. However, his data shows the resistance to be

more frequency dependent at the low flow rates than that presented in Figure 15. Figure 16 shows that for the higher POA perforate samples the resistance is more dependent on frequency. This concurs with Premo's results.

A limited investigation into the effects of negative bias flow (suction) was also conducted. Due to vacuum pump constraints, only low negative flow rates could be achieved. Figure 17 shows a comparison between the impedances at 0, +25 and -25 cm/s (no flow, blowing and suction, respectively). The acoustic resistance was consistently lower for suction than for blowing for all perforates and SPL's tested. Reactance was unaffected by the direction of the flow.

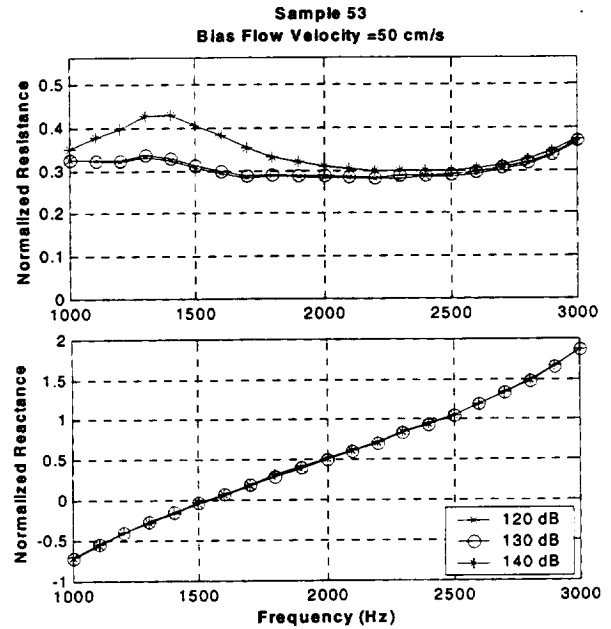


Figure 12. Measured impedance of perforate 53. Varying SPL at 50 cm/s incident bias flow.

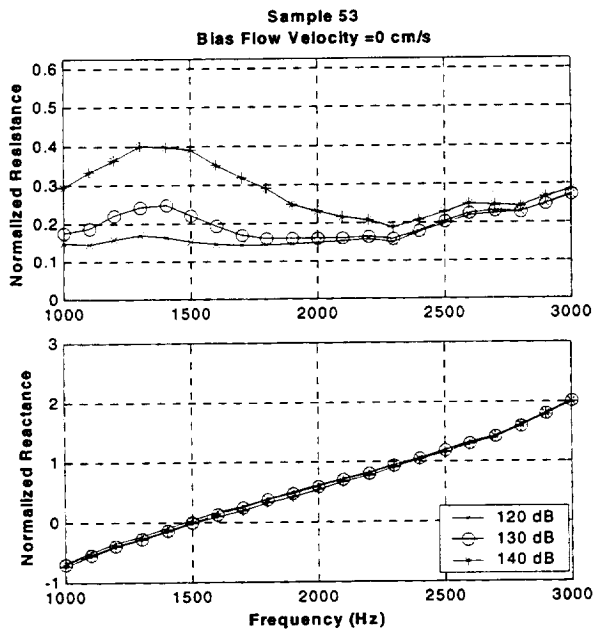


Figure 11. Measured impedance of perforate 53. Varying SPL with no bias flow.

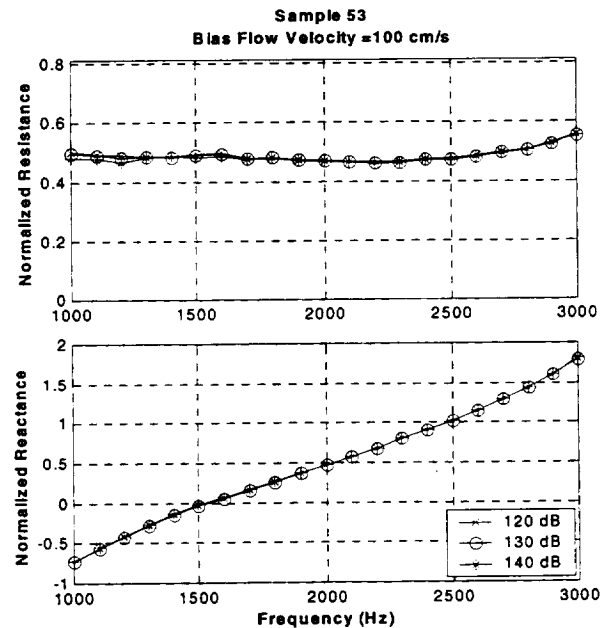


Figure 13. Measured impedance of perforate 53. Varying SPL at 100 cm/s incident bias flow.

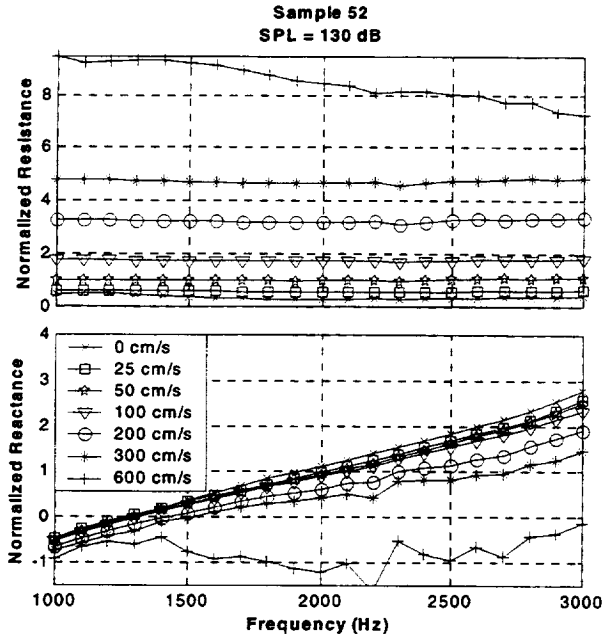


Figure 14. Measured impedance of perforate sample 52. Constant SPL of 130 dB, increasing bias flow.

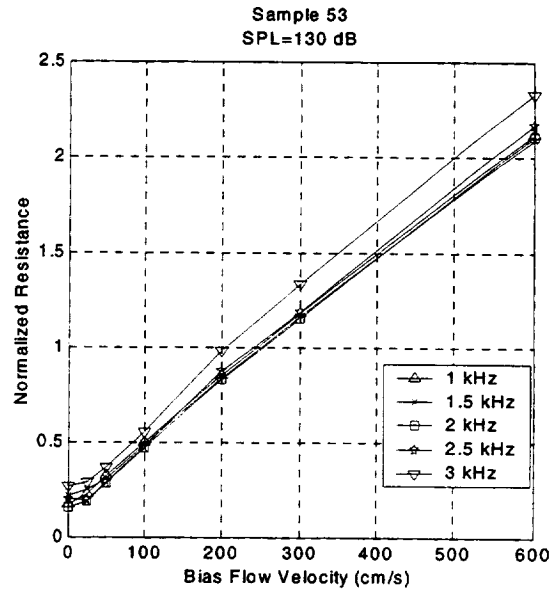


Figure 16. Resistance data for perforate sample 53 with increasing bias flow rate for several frequencies at constant SPL of 130 dB.

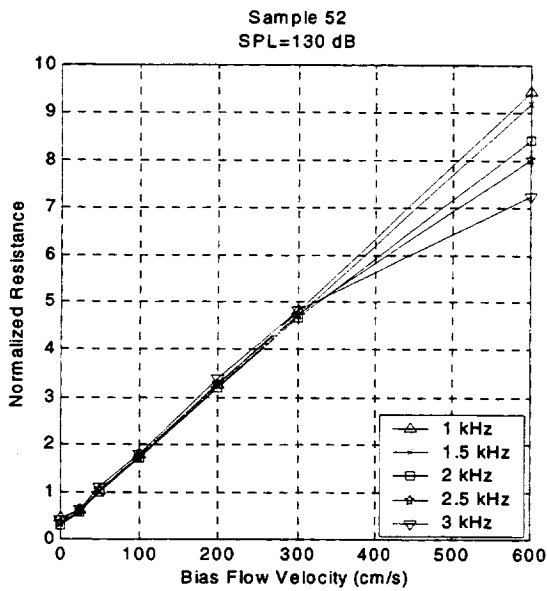


Figure 15. Resistance data for perforate sample 52 with increasing bias flow rate for several frequencies at constant SPL of 130 dB.

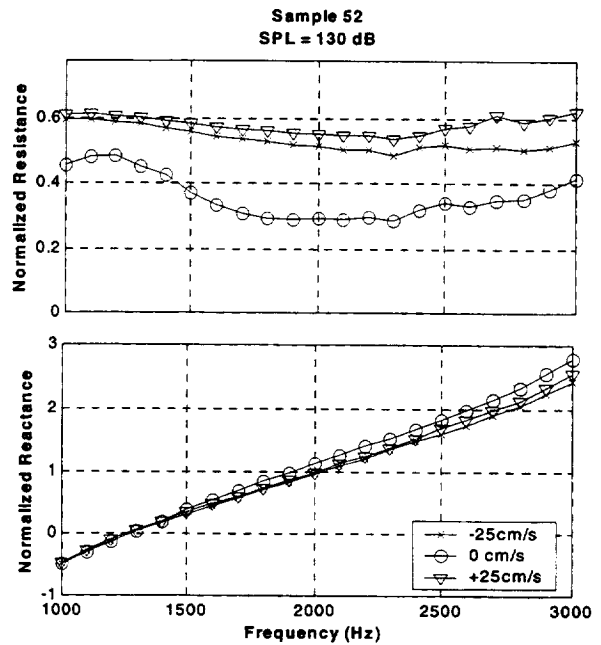


Figure 17. Measured impedance of perforate sample 52. Comparing difference between negative (suction) and positive (blowing) bias flow at constant SPL of 130 dB.

Conclusions

The normal incidence impedance was measured for a series of perforated plate liners with varying thickness, hole diameters, percent open areas, and bias flow rates using the NASA Langley Normal Incidence Tube (NIT).

A method was devised to introduce a bias flow through the tested liners without introducing unknown cavity impedance. This was accomplished with the use of a high resistance fibermetal termination, which maximized sound reflection while allowing the passage of a mean bias flow through the liner. Plate resonance was eliminated from the testing frequency range by adding a post support mechanism that increased the plate stiffness element.

The original fixed microphone technique developed by Chung and Blazer was adapted for this study for the purpose of eliminating the need for microphone switching. A modification of a microphone switching technique previously in use in the NIT was used to efficiently implement high quality microphone calibrations. This combination provided the basis of high-quality transfer function measurements needed for the normal incidence impedance determination.

The results of the normal incidence impedance tests conducted on the series of perforated plate liners can be summarized as follows:

1. A quality database has been acquired that will be useful in bias flow model development.
2. Increasing bias flow tends to increase resistance and decrease the slope of the reactance.
3. Bias flow reduces the nonlinearity of perforated liners above a critical flow rate. This critical flow rate is perforate and SPL dependant.
4. Bias flow reduces the variation of resistance with frequency.
5. Negative bias flow (suction) provides consistently lower resistance than positive bias flow (blowing) of equal magnitude.

A possible new design feature for maximizing future liner performance is to allow in-situ adjustment of liner impedance. The results presented in this study indicate that bias flow may be capable of providing this capability. In addition, the ability to change the slope of the reactance and decrease the nonlinearity effects of resistance offer the potential to control the liner impedance in such a way as to achieve optimum absorption values.

Acknowledgments

The authors gratefully acknowledge funding for this research from the Structural Acoustics Branch of NASA Langley Research Center. The support of Mike Jones, Tony Parrott, Houston Wood and Carol Winbush was essential to the completion of this research.

References

1. Kelly, J.J., Betts, J.F., Follet, J.I., and Thomas, R.H., "Bias Flow Liner Investigation", Virginia Tech Report, VPI-434487, December 1999.
2. Premo, J., "The Application of a Time-Domain Model to Investigate the Impedance of Perforate Liners Including the Effects of Bias Flow", AIAA Paper No. 99-1876, Presented at the Fifth AIAA/CEAS Aeroacoustics Conference, May 1999.
3. Cataldi, P., Ahuja, K.K., and Gaeta, R.J., "Enhanced Sound Absorption Through Negative Bias Flow", AIAA Paper No. 99-1879, Presented at the Fifth AIAA/CEAS Aeroacoustics Conference, May 1999.
4. Betts, J.F., Follet, J.I., Kelly, J.J., and Thomas, R.H., "Evaluation of an Impedance Model for Perforates Including the Effect of Bias Flow", AIAA Paper No. 2000-1949, Presented at the Sixth AIAA/CEAS Aeroacoustics Conference, June 2000.
5. Jones, M.G. and Parrott, T.L., "Evaluation of a Multi-point Method for Determining Acoustic Impedance", *Mechanical Systems and Signal Processing*, 3(1), 1989, pp. 15-35.
6. Jones, M.G., and Steide, P.E., "Comparison of Methods for Determining Specific Acoustic Impedance", *J. Acoust. Soc. Am.* (5), Pt.1, May 1997.
7. Melling, T.H., "The Acoustic Impedance of Perforates at Medium and High Sound Pressure Levels", *J. Sound and Vibration.* (29), Pt.1, 1973.
8. Chung, J.Y., and Blaser, D.A., "Transfer Function Method Of Measuring In-Duct Acoustic Properties: II. Experiment", *J. Acoust. Soc. Am.* (68), Pt.3, 1980.
9. Seybert, A.F., and Ross, D.F., "Experimental Determination Of Acoustic Properties Using A Two-Microphone Random-Excitation Technique", *J. Acoust. Soc. Am.* (61), Pt.5, 1977.
10. Doebelin, E.O., *Measurement Systems: Application and Design*, McGraw-Hill, Inc., New York, 1990.

